Cancer Research

# Development of a Lung Cancer Therapeutic Based on the Tumor Suppressor MicroRNA-34

Jason F. Wiggins, Lynnsie Ruffino, Kevin Kelnar, Michael Omotola, Lubna Patrawala, David Brown, and Andreas G. Bader

## Abstract

Tumor suppressor microRNAs (miRNA) provide a new opportunity to treat cancer. This approach, "miRNA replacement therapy," is based on the concept that the reintroduction of miRNAs depleted in cancer cells reactivates cellular pathways that drive a therapeutic response. Here, we describe the development of a therapeutic formulation using chemically synthesized miR-34a and a lipid-based delivery vehicle that blocks tumor growth in mouse models of non–small-cell lung cancer. This formulation is effective when administered locally or systemically. The antioncogenic effects are accompanied by an accumulation of miR-34a in the tumor tissue and downregulation of direct miR-34a targets. Intravenous delivery of formulated miR-34a does not induce an elevation of cytokines or liver and kidney enzymes in serum, suggesting that the formulation is well tolerated and does not induce an immune response. The data provide proof of concept for the systemic delivery of a synthetic tumor suppressor mimic, obviating obstacles associated with viral-based miRNA delivery and facilitating a rapid route for miRNA replacement therapy into the clinic. *Cancer Res; 70(14); 5923–30. ©2010 AACR.*

## Introduction

MicroRNAs (miRNA) are small noncoding, naturally occurring RNA molecules that posttranscriptionally modulate gene expression and determine cell fate by regulating multiple gene products and cellular pathways (1). Misregulation of miRNAs is often a dire cellular event that can contribute to the development of human diseases including cancer (2, 3). miRNAs deregulated in cancer target multiple oncogenic signaling pathways and have therefore the potential of becoming powerful therapeutic agents (4, 5). Among the miRNAs expressed at reduced levels in various human cancer types is miR-34a (6–11). miR-34a is a member of the miR-34 family, which is composed of miR-34a, miR-34b, and miR-34c. The *miR-34a* gene is located on chromosome 1p36.22 in a region that has previously been associated with various cancers including lung cancer (12). In addition, frequent hypermethylation of the miR-34a promoter is another mechanism that can lead to reduced miR-34a expression in lung cancer and other cancer types (7, 11). miR-34a is transcriptionally induced by the tumor suppressor p53 (6, 13–16), and low miR-34a expression levels correlate with a high probability of relapse in non–small-cell lung cancer (NSCLC) patients (11). Overexpression of miR-34a inhibits the growth of cultured cancer cells and affects gene products that promote cell cycle progression and counteract apoptosis (6, 13–16). miR-34a also inhibits the growth of pancreatic cancer stem cells (17). Thus, miR-34a displays an antiproliferative phenotype in numerous cancer cell types (6, 13–16). However, the antioncogenic activity of miR-34a *in vivo* and its potential as a therapeutic remain unknown. Here, we show the tumor suppressor function of miR-34a *in vivo* and evaluate the therapeutic activity of a synthetic miR-34a mimic in an effort to restore a loss of function in cancer.

**Authors' Affiliation:** Mirna Therapeutics, Inc., Austin, Texas

**Note:** Supplementary data for this article are available at Cancer Research Online (http://cancerres.aacrjournals.org/).

**Corresponding Author:** Andreas G. Bader, Mirna Therapeutics, 2150 Woodward Street, Suite 100, Austin, TX 78744. Phone: 512-681-5200; Fax: 512-681-5201; E-mail: abader@mirnarx.com.

**doi:** 10.1158/0008-5472.CAN-10-0655



## Materials and Methods

### Human tissue samples, cell lines, and oligos

Thirteen flash-frozen NSCLC tumor samples and corresponding normal adjacent tissues (NAT) were purchased from ProteoGenex; five flash-frozen tissue pairs were purchased from the National Disease Research Interchange. All 14 formalin-fixed paraffin-embedded (FFPE) lung tumor samples and NATs were acquired from Phylogeny/Folio Biosciences. All lung cancer cell lines were purchased from the American Type Culture Collection and cultured according to the vendor's instructions: A549, BJ, NCI-H460, Calu-3, NCI-H596, NCI-H1650, HCC2935, SW-900, NCI-H226, NCI-H522, NCI-H1299, Wi-38, and TE353.sk. Primary T cells were obtained from Atlanta Pharmaceuticals. Transfection and proliferation assays were carried out as described (18, 19), and proliferation was assessed using Alamar Blue (Invitrogen) 3 to 7 days after transfection depending on the growth rates of individual cell lines. Cellular viability was determined using Neutral Red from Sigma-Aldrich following the manufacturer's instructions. For colony formation assays, $5 \times 10^6$ cells were electroporated with 1.6 μmol/L miRNA in 200 μL of OptiMEM (Invitrogen) using

the Bio-Rad GenePulserXcell instrument, and 3,000 cells were seeded on 100-mm dishes. After 32 days, colonies were stained with 2% crystal violet and colonies containing >50 cells were counted. Synthetic miRNAs and siRNAs were obtained from Ambion, Applied Biosystems and Dharmacon, Thermo Scientific.

### Quantitative real-time PCR analysis

Total RNA from flash-frozen NSCLC tumors and normal adjacent tissues, as well as human lung cancer cells and tumor xenografts, was isolated using the mirVANA PARIS RNA isolation kit (Ambion) following the manufacturer's instructions. Total RNA from FFPE tissues was isolated using the RecoverAll Kit from Ambion. For quantitative real-time PCR (RT-PCR) detection of the miR-34a oligonucleotide, 10 ng of total RNA and miR-34a–specific RT-primers [assay ID 000426, TaqMan miRNA Assay, Applied Biosystems (ABI)] were heat-denatured at 70°C for 2 minutes and reverse-transcribed using Moloney murine leukemia virus reverse transcriptase (Invitrogen). The housekeeping miRNAs miR-191 and miR-103 (ABI assay IDs 002299 and 000439) were amplified as internal references (20) to adjust for well-to-well RNA input variances. For detection of mouse *IFIT1* mRNA levels in mouse lung tissue, cDNA was generated by random decamers (Ambion) using 10 ng of total RNA under the conditions described above and amplified using a TaqMan Gene Expression Assay (ABI assay ID Mm00515153_m1). Raw CT values were normalized to the values of murine glyceraldehyde-3-phosphate dehydrogenase (GAPDH; Integrated DNA Technologies) to correct for equal input of RNA. For detection of human TP53, $p21^{WAF1/CIP1}$, and MDM2 in NSCLC tissues, cDNA was generated by random decamers using 500 ng of total RNA under the conditions described above and amplified using the TaqMan Gene Expression Assays Hs99999147_m1 (TP53), Hs00355782_m1 (p21), and Hs99999008_m1 (MDM2). Raw Ct values were normalized to the geometric mean of PPIA (amplified using ABI assay Hs99999904_m1), GAPDH (amplified using ABI assay Hs99999905_m1), and 18S (amplified using ABI assay Hs99999901_s1). All gene expression levels were determined by real-time PCR using Platinum Taq Polymerase reagents (Invitrogen) and the ABI Prism 7900 SDS instrument (Applied Biosystems).

### Lung cancer xenografts

All animal experiments were performed in accordance with currently prescribed guidelines and under a protocol approved by the Institutional Animal Care and Use Committee at BIOO Scientific Corporation. H460 and A549 NSCLC cells were collected, counted, and mixed with Matrigel (BD Biosciences) in a 1:1 ratio by volume. Cells ($3 \times 10^6$) in 100 μL of medium/Matrigel solution were injected s.c. in the lower back region of female nonobese diabetic/severe combined immunodeficient (NOD/SCID) mice (The Jackson Laboratory). Tumor volumes were determined as previously described (18). miRNA (100 or 20 μg) was formulated with MaxSuppressor *in vivo* RNALancerII, a lipid-based delivery reagent (BIOO Scientific, Inc.), according to the manufacturer's instructions. Formulated miRNA was administered intratumorally (i.t.) or intravenously (i.v.) by tail vein injections once tumors reached a volume of 150 to 200 $mm^3$. Tumors and organs were collected, split, and placed in either 10% formalin for histology or homogenized in 1× denaturing solution (Ambion) for RNA isolation.

### Tumor histology and immunohistochemistry

Tumor tissues were fixed in formalin and embedded in paraffin using the Microm Tissue Embedding Center (Labequip, Ltd.). Sections (5 μm) were cut and stained with H&E. For immunohistochemical staining, sections were deparaffinized and hydrated, and endogenous peroxidase activity was blocked with 3% $H_2O_2$ in water for 10 minutes. Antigen retrieval was done with 10 mmol/L citrate buffer (pH 6.0) for 10 minutes in a microwave oven followed by a 20-minute cooldown and thorough washing in TBS with Tween 20 [TTBS; 50 mmol/L Tris-HCl (pH 7.4), 150 mmol/L NaCl, 0.1% Tween 20]. Slides were incubated with Biocare blocking reagent (with casein in the buffer; Biocare Medical) for 10 minutes to block nonspecific binding. Slides were incubated with various primary antibodies directed against ki67 (DAKO), caspase-3 (R&D Systems), c-Met, cyclin-dependent kinase 4 (CDK4), and Bcl-2 (Santa Cruz Biotechnology) for 30 minutes at room temperature. Slides were washed in TTBS twice and then incubated in biotinylated goat anti-rabbit or goat anti-mouse IgG (Vector Laboratories) at 1:500 dilution for 30 minutes at room temperature. After washing, slides were incubated with antigoat horseradish peroxidase–conjugated secondary antibodies (BioGenex) for 30 minutes at room temperature and then washed. Finally, slides were incubated with 3,3′-diaminobenzidine (BioGenex Laboratories) and color development was closely monitored under a microscope. Slides were counterstained with hematoxylin.

### Cytokines and blood chemistries

Female BALB/c mice (The Jackson Laboratory) were injected i.v. in a lateral tail vein with 100 μg of miRNA formulated with MaxSuppressor *in vivo* RNALancerII. As a positive control for cytokine induction, a group of animals were injected with 20 μg of lipopolysaccharide (LPS) from *Escherichia coli* 0111:B4 (Sigma-Aldrich). Mice were anesthetized with isoflurane using a Laboratory Animal Anesthesia System (VetEquip) and blood was collected via cardiac stick at set time points after injection into a serum separator tube for serum isolation or into an EDTA tube (Sarstedt) for whole blood chemistry analysis. Serum cytokine levels were determined using a mouse Fluorokine Multianalyte Profiling Kit (R&D Systems) and the Luminex 100 IS instrument. For blood chemistry analysis, whole blood was sent to the Comparative Pathology Laboratory at UC Davis.

## Results

### miR-34a is suppressed in human NSCLC tissues

To assess the expression levels of miR-34a in patients with NSCLC, we have tested a cohort of 18 human tumor samples that were flash-frozen after biopsy and a cohort of 14 tumor samples that were formalin-fixed and paraffin-embedded (FFPE) before RNA isolation. The sample collection was

composed of the predominant histotypes of NSCLC, including 9 adenocarcinoma, 17 squamous cell carcinoma, 4 large cell carcinoma, and 2 bronchioalveolar carcinoma (Supplementary Table S1). Expression levels in the tumor tissue were assessed by quantitative RT-PCR and compared with the levels in the corresponding NATs (Fig. 1). Of the 32 tumor samples, 20 (63%) showed reduced miR-34a expression with an average expression level that is 60% of the expression observed in the corresponding normal adjacent lung samples. Reduced miR-34a was observed in all histotypes of NSCLC, in agreement with other reports showing downregulation of miR-34a in a broad range of tumor types including lung cancer (6, 7, 11). Tumor levels of miR-34a did not correlate with disease stage (Supplementary Table S1). Similar to tumor tissues, established NSCLC cell lines frequently showed a reduction in miR-34a levels (Fig. 1). The ones devoid of miR-34a expression carry mutations in the *p53* gene (H1299, H522, H596, Calu-3, and SW-900; refs. 21, 22) in accord with previous data showing that miR-34a is a transcriptional target of p53 (6, 13–16).

To correlate miR-34a expression levels with the transcriptional activity of p53 in human tumors, we determined the mRNA levels of $p21^{WAF1/CIP1}$ and MDM2, both of which are transcriptionally induced by p53 and have previously been used as a measure for p53 activity (23–25). Thus, reduced p53 activity could be reflected by reduced levels of MDM2 and $p21^{WAF1/CIP1}$ in the tumor tissue relative to NAT. However, other factors potentially contributing to the expression levels of these targets must be considered. The analysis was limited to 15 RNA samples generated from flash-frozen tissues, as RNA from FFPE samples does not exert RNA qualities that are sufficient to assess mRNA levels. Although no significant correlation was observed between p53 activity and miR-34a levels ($R^2_{p21/miR\text{-}34a}$ = 0.2094, $R^2_{MDM2/miR\text{-}34a}$ = 0.1495), all tumors with reduced miR-34a expression also showed reduced mRNA levels of $p21^{WAF1/CIP1}$ and MDM2 (Supplementary Table S1). Similar results on p53 mutation status and miR-34a levels in NSCLC have been reported by Gallardo and colleagues (11). As anticipated, p53 mRNA levels did not correlate with those of its targets ($R^2_{p53/p21}$ = 0.0392, $R^2_{p53/MDM2}$ = 0.0692), in agreement with the observation that p53 levels are not indicative of its functional status (Supplementary Table S1; refs. 25–27).

## miR-34a inhibits the growth of cultured lung cancer cells

The data suggest that suppression of miR-34a might be critical in acquiring a malignant phenotype and that reintroduction of miR-34a may interfere with the oncogenic properties of NSCLC cells. To test this possibility, we transiently transfected a panel of NSCLC cell lines with miR-34a and measured proliferation after 72 hours. The human NSCLC cell lines chosen vary in histology and cancer genotype and therefore allow an evaluation of miR-34a–induced effects in a genetically diverse set of NSCLC (22). As a control, cancer cells were transfected separately with a negative control miR-NA (miR-NC) that contains a scrambled sequence and does not specifically target any human gene products (Ambion). As an indication for successful transfection and extent of growth inhibition, cells were transfected with an siRNA directed against the spindle protein kinesin 11 (EG5; Supplementary Fig. S1A; ref. 28). As shown in Fig. 2A, most cancer cell lines exhibited reduced cell growth in the presence of miR-34a. The degree of growth inhibition is similar to those of other lung cancer–directed therapies in transient cell assays (29). Cells transfected with miR-34a showed signs of stress as evidenced by a loss of the spindle-like shape followed by either rounding and detachment or a large, flat senescence-like phenotype (Supplementary Fig. S2).

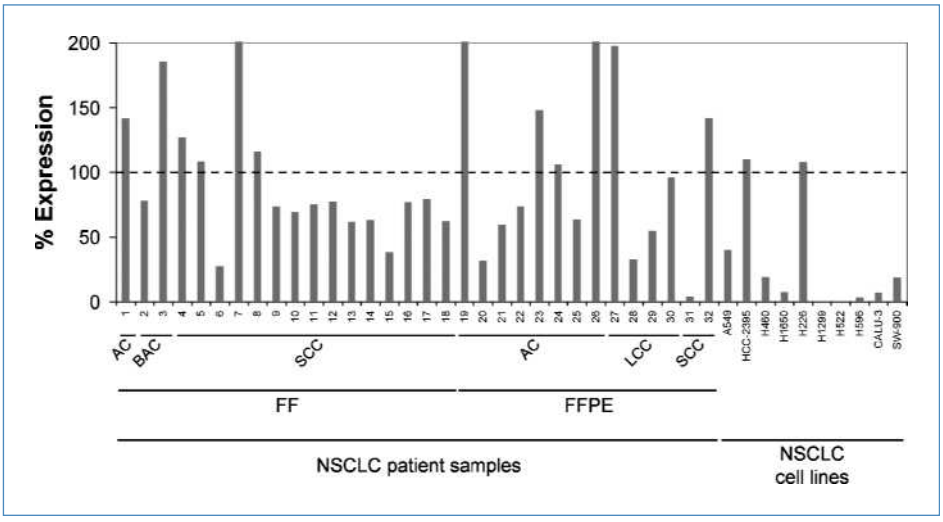


**Figure 1.** miR-34a expression in human NSCLC. Quantitative RT-PCR analysis of miR-34a using total RNA from 32 NSCLC tumor samples and their corresponding NATs, as well as total RNA from various NSCLC cell lines. Raw Ct values from lung tumors and NATs were normalized to a housekeeping miRNA (20) and expressed as percent expression compared with levels in the respective NATs from the same patient (100%). Values derived from cell lines were compared with the expression value in Wi-38 normal lung fibroblasts (100%). FF, flash-frozen; FFPE, formalin-fixed paraffin-embedded; AC, adenocarcinoma; BAC, bronchioalveolar carcinoma; LCC, large cell carcinoma; SCC, squamous cell carcinoma.

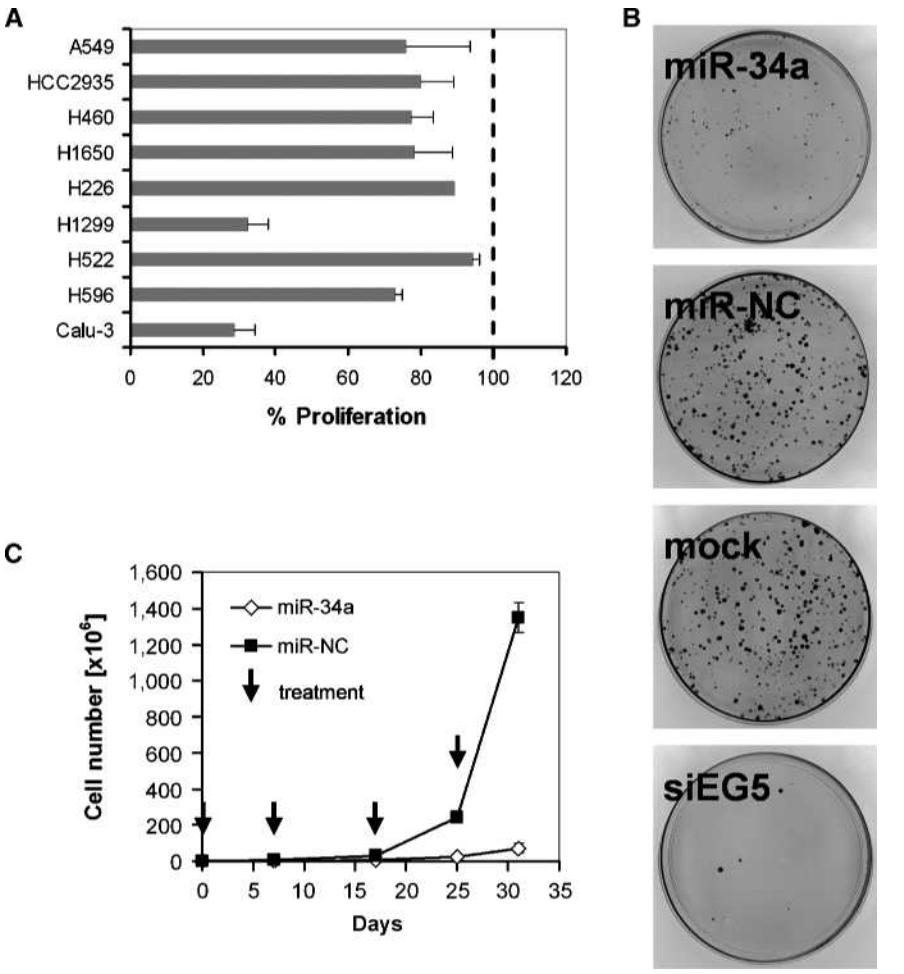


**Figure 2.** Inhibitory activity of miR-34a in cultured lung cancer cells. A, transient effects of synthetic miR-34a. Cancer cell lines were transfected in triplicate with 30 nmol/L miR-34a or miR-NC. Proliferation was assessed 3 to 7 d after transfection using Alamar Blue (Invitrogen). Percent change in proliferation was plotted relative to proliferation of miR-NC–transfected cells. Columns, average of three replicates; bars, SD. B, colony formation assay using SW-900 lung cancer cells. Cells were transfected with synthetic miR-34a, miR-NC, and siEG5 siRNA and seeded at 3,000 cells per 100-mm dish. After 32 d, cells were stained with 2% crystal violet. Colonies containing >50 cells were counted. C, long-term effects of miR-34a. H226 cells were transfected in triplicate with miR-34a and miR-NC, seeded, and propagated in regular growth medium. When the control cells reached confluence, cells were harvested, counted, and transfected again with the respective miRNAs. The population doublings were calculated, and cell counts were extrapolated and plotted on a linear scale. Arrows, transfection events. Points, average cell counts of three replicates; bars, SD. Cell lines carrying mutated p53 include Calu-3, H596, H1299, H522, and SW-900 (21, 22). A549 and H460 carry wild-type p53 (21, 22).

Interestingly, the inhibitory effects of exogenous miR-34a were not limited to cell lines with reduced endogenous miR-34a expression and also affected cell lines with normal miR-34a expression levels (e.g., H226 cells; Fig. 1). Inhibition of cancer cell growth by miR-34a was also independent of p53 status (Fig. 2A). A colony formation assay using SW-900 cells carrying mutated p53 further shows the ability of miR-34a to inhibit the proliferation of NSCLC cells in the absence of functional p53 (Fig. 2B). Colony formation of cells transfected with miR-34a was merely 9% relative to cells transfected with miR-NC (100%) 32 days after transfection. SW-900 cells proliferate considerably slower than most other NSCLC cells, and therefore, we speculate that the miR-34a mimic is less rapidly subject to dilution due to ongoing cell divisions compared with fast-dividing cells, which might explain the extended duration of miR-34a activity in SW-900 cells (30, 31). To study the long-term effects of miR-34a in rapidly dividing cells, we serially transfected miR-34a into H226 lung cancer cells, a cell line that moderately responded to miR-34a in transient transfection experiments. Cell counts were taken during the experiment and extrapolated to calculate population doublings and final cell numbers. miR-NC–treated cells showed normal exponential growth (Fig. 2C). In contrast, miR-34a severely retarded H226 cancer cell proliferation. To assess whether the inhibitory effects of miR-34a were specific to cancer cells, we measured the proliferation effects of miR-34a in nonmalignant cell lines including normal Wi-38 lung fibroblasts. In contrast to cancer cells, transient transfection of miR-34a into nonmalignant cell lines had no effect on their ability to proliferate (Supplementary Fig. S1B). Similarly, a direct comparison of the cellular viability of A549 lung cancer cells versus normal BJ cells in response to increasing miR-34a concentrations indicated that normal cells are more refractory to miR-34a than cancer cells (Supplementary Fig. S1C). In summary, the data suggest that miR-34a exerts an antireplicative function in a broad range of lung cancer cells.

### Intratumoral delivery of formulated miR-34a blocks lung tumor growth in mice

We next investigated whether administration of synthetic miR-34a could block lung tumor growth in the animal. Naked

miRNA oligonucleotides are rapidly degraded in biofluids, and therefore, we formulated the miRNA in a lipid-based delivery vehicle that is designed for systemic delivery of the oligonucleotide to various tissues (Materials and Methods). Because the range of an effective systemically administered miRNA dose and the rate of successful delivery to the tumor tissue were unknown, we first evaluated the miR-34a–induced effects of i.t. injections using 100 μg of oligo, which corresponds to a relative concentration sufficient to induce growth inhibitory effects in cultured cancer cells. H460 NSCLC cells, a fast-growing tumor xenograft that yields large tumors within 3 weeks after implantation, were grafted s.c. into the lower back of NOD/SCID mice and grown until palpable tumors formed. On day 12 after xenograft implantation, a group of tumor-bearing mice received i.t. injections of formulated miR-34a. Local injections were repeated on days 15 and 18 to maintain increased levels of miR-34a in the tumor tissue. As controls, a separate group of animals were injected i.t. with PBS, the vehicle only, or vehicle formulated with miR-NC. As shown in Fig. 3A, tumors injected with formulated miR-NC were unaffected and developed at a pace similar to those that received PBS or vehicle. In contrast, i.t. injections of formulated miR-34a prevented the outgrowth of viable tumors. A histologic analysis revealed that miR-34a–treated tumors contained large areas filled with cell debris (Fig. 3B). The few seemingly viable tumor cells that remained preferentially in the periphery of the tumor showed reduced expression of ki67 and an increase in caspase-3, indicating that miR-34a actively inhibits proliferation and stimulates the apoptotic cascade in H460 tumor cells. To better correlate the activity of miR-34a, we measured the protein levels of endogenous CDK4 and c-Met, both of which are directly repressed by miR-34a (13). Tumors treated with miR-34a lacked the expression of CDK4 and c-Met relative to tumors that received miR-NC (Fig. 3C). Similarly, Bcl-2, another direct target of miR-34a (6), was repressed in tumors that received formulated miR-34a (Supplementary Fig. S3). The downregulation of CDK4, c-Met, and Bcl-2 demonstrates the specific activity of miR-34a in H460 tumor cells; however, we assume that the regulation of other targets is necessary to explain the complete miR-34a phenotype. The expression of miR-34a targets inversely correlated with ~100-fold increased miR-34a levels in the tumor tissue relative to endogenous miR-34a levels in H460 tumor cells (Fig. 3D). The data suggest that local administration of formulated miR-34a induces a specific inhibitory effect in tumor cells with an accumulation of miR-34a and concurrent repression of its direct target genes.

### Systemic delivery of formulated miR-34a inhibits the growth of established lung tumors *in vivo*

To evaluate the miR-34a–dependent effects on systemic delivery of the miRNA, we repeated the experimental framework using the H460 xenograft. Animals carrying palpable subcutaneous tumors were treated with formulated miR-34a, miR-NC, or vehicle only. In contrast to the previous study, however, formulations were administered by i.v. tail vein injections. Each dose contained 100 μg of formulated oligo, which equals 5 mg/kg per mouse with an average weight of 20 g. Similar to i.t. injections of miR-34a, repeated i.v. delivery of formulated miR-34a specifically blocked tumor growth (Fig. 4A). Tumor tissues from miR-34a–treated animals frequently showed areas with cell debris, reduced expression of ki67, and an increase in caspase-3 (Fig. 4B), in agreement with the effects induced by local delivery of miRNA. Systemic delivery of formulated miR-34a at 1 mg/kg also inhibited the growth of established A549 NSCLC xenografts, further showing the antitumor activity of miR-34a (Supplementary Fig. S4A). The histology and immunohistochemical staining of A549 tumors that received miR-34a resemble those of

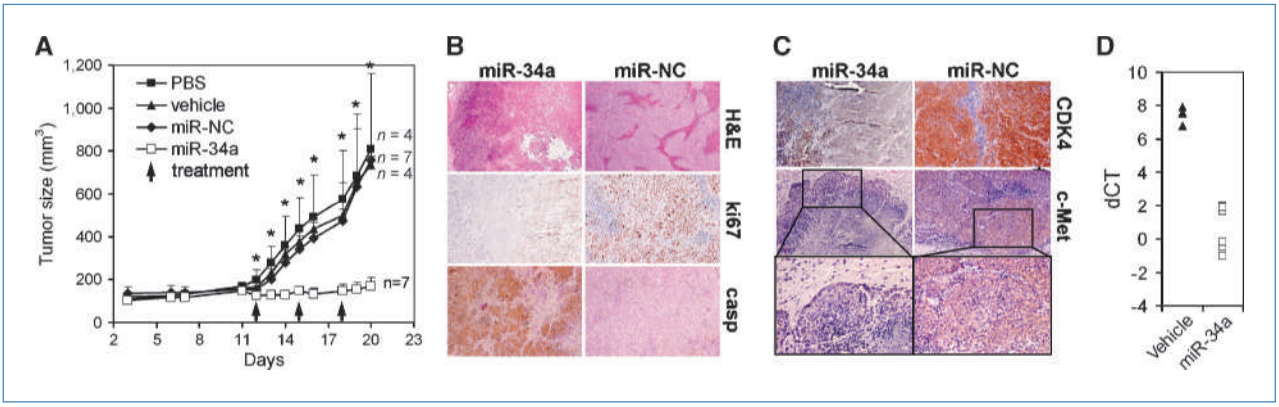


Figure 3. Local delivery of formulated miR-34a inhibits lung tumor growth in mice. A, effects of formulated miR-34a in H460 tumors by i.t. injections. Palpable subcutaneous H460 tumor xenografts were treated on days 12, 15, and 18 with each 100 μg of formulated miR-34a or miR-NC. As controls, separate groups of tumor-bearing animals were injected with vehicle alone or PBS. Caliper measurements were taken on the days indicated and averaged. Bars, SD. **, $P < 0.05$; *, $P < 0.01$, miR-34a versus miR-NC (Student's $t$ test, two-tailed). B and C, histologies and immunohistochemical stainings directed against ki67, caspase-3, CDK4, and c-Met in H460 tumors after sacrifice. Histologies at 100-fold magnification and immunohistochemical stainings at ~300-fold magnification are shown. Insets, c-Met–specific stainings at 400-fold magnification. D, quantitative RT-PCR analysis of miR-34a in H460 tumors treated with formulated miR-34a or vehicle after sacrifice. Raw Ct values from lung tumors and NATs were normalized to a housekeeping miRNA (20) and expressed as dCT [log 2].

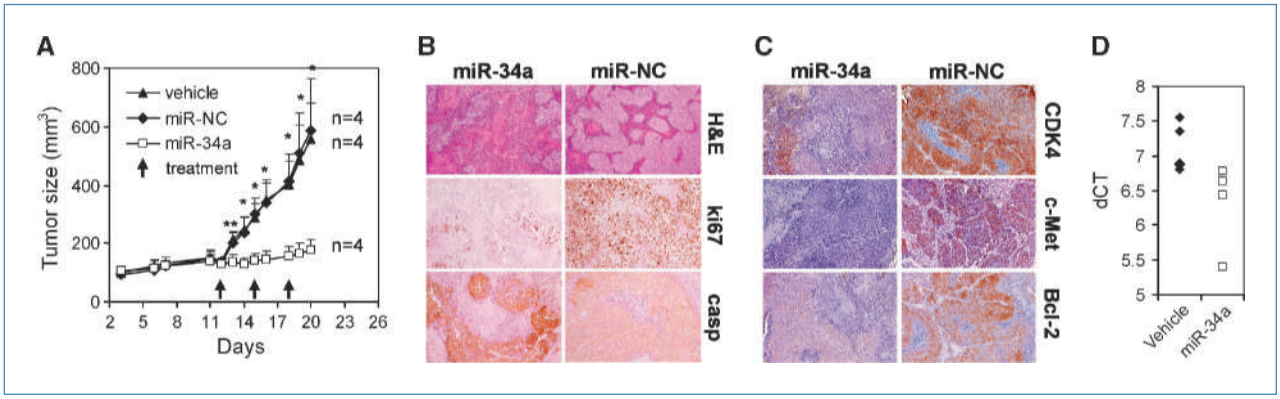


Figure 4. Intravenous delivery of formulated miR-34a blocks the growth of human lung tumors in mice. A, mice carrying palpable subcutaneous H460 tumor xenografts were treated on days 12, 15, and 18 with lipid-formulated miR-34a, miR-NC, vehicle alone, or PBS by i.v. tail vein injections. Each dose contained 100 μg of formulated oligo. Caliper measurements were taken on the days indicated and averaged. Bars, SDs. **, $P < 0.05$; *, $P < 0.01$, miR-34a versus miR-NC (Student's $t$ test, two-tailed). B and C, histologies and immunohistochemical stainings specific for ki67, caspase-3, CDK4, c-Met, and Bcl-2 in H460 tumors after sacrifice. Histologies at 100-fold magnification and immunohistochemical stainings at ~300-fold magnification are shown. D, quantitative RT-PCR analysis of miR-34a in H460 tumors treated with formulated miR-34a or vehicle after sacrifice. Raw Ct values from lung tumors and NATs were normalized to a housekeeping miRNA (20) and expressed as dCT [log 2].

treated H460 tumors, suggesting that repeated administration of a miR-34a mimic inhibits proliferation and induces apoptosis in A549 lung tumor cells (Supplementary Fig. S4B). Similar to local administration of miR-34a, the growth inhibitory effects correlated with an accumulation of miR-34a in the tumor tissue and repression of c-Met and Bcl-2, as well as partial repression of CDK4 (Fig. 4C and D). However, the overall abundance of systemically delivered miR-34a in the tumor tissue was substantially less compared with locally delivered oligo and suggests that only minimal amounts of miR-34a are needed to elicit a therapeutic effect. Interestingly, the tumors with the greatest suppression of miR-34a targets were also the ones with the highest accumulation of miR-34a oligonucleotide.

### Systemic delivery of formulated miR-34a does not lead to elevated blood chemistries nor trigger an immune response

To assess the safety profile of systemically delivered miR-34a, we examined serum levels of alanine aminotransferase,

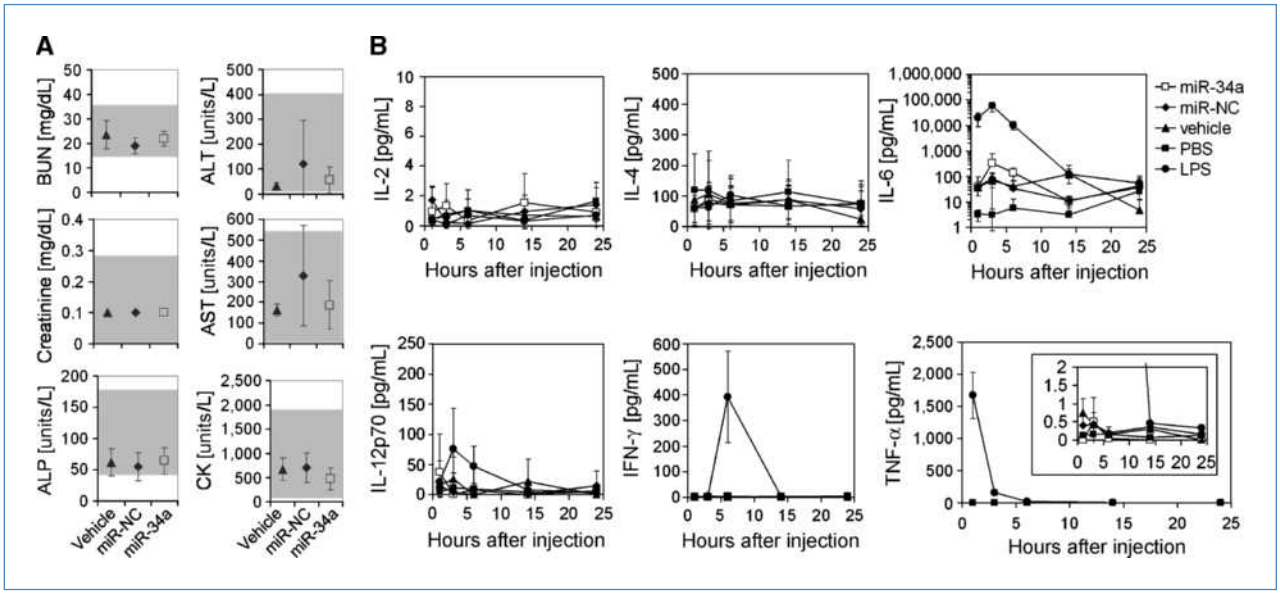


Figure 5. Blood chemistries and cytokine levels in response to systemic delivery of formulated miR-34a. A, serum levels of blood urea nitrogen (BUN), creatinine, alkaline phosphatase (ALP), alanine aminotransferase (ALT), aspartate aminotransferase (AST), and creatine kinase (CK) of the animals described in Fig. 4A after sacrifice. Points, average of four animals; bars, SD. The gray-shaded area indicates guideline ranges as reported by the Comparative Pathology Laboratory at UC Davis. B, serum cytokine levels in immunocompetent BALB/c mice 1 to 24 h after i.v. injection of a single dose of formulated miR-34a, miR-NC, vehicle, and PBS. LPS was used as a positive control for IL-6, IFN-γ, and TNF-α induction. Points, average of three animals per group; bars, SD. IL-6 data are shown on a logarithmic scale.

aspartate aminotransferase, blood urea nitrogen, alkaline phosphatase, creatinine, and creatine kinase from mice repeatedly treated with formulated miR-34a, miR-NC, or vehicle alone. As shown in Fig. 5A, the values of these blood chemistries, which would indicate toxicity in liver, kidney, and heart, were within the reference range and suggested that miRNA treatment was well tolerated. To determine whether the antioncogenic effects of miR-34a are indeed a specific consequence of the miRNA and not the result of a nonspecific induction of the immune system, we measured serum cytokine levels in immunocompetent BALB/c mice (Fig. 5B). An activation of the immune system has been reported previously to be induced by other oligonucleotide-containing formulations that might, at least in part, contribute to the effects of the therapeutic (32–35). Because a burst of cytokines usually occurs within just a few hours after administration of the stimulant, we evaluated cytokine levels 1 to 24 hours after i.v. administration of formulated miRNA (36–38). As a positive control, a group of mice were i.v. injected with a nonlethal dose of 1 mg/kg LPS (39), which stimulated an induction of interleukin (IL)-6, tumor necrosis factor α (TNF-α), and IFN-γ (Fig. 5B). These LPS-treated mice also developed acute signs of illness, such as hunched posture, ruffled coat, and labored movement, and fully recovered within 24 hours after injection. In contrast, formulated miR-34a, miR-NC, or the vehicle control failed to induce an immune response as evidenced by normal serum levels of IL-2, IL-4, IL-12, IFN-γ, and TNF-α (Fig. 5B), as well as normal levels of IL-1β and IL-5 (Supplementary Fig. S5) 1 to 24 hours after i.v. injection. Similarly, mRNA levels of *IFIT1*, a gene induced by IFN-α, were solely elevated in response to LPS (Supplementary Fig. S6). IL-6, a pro- and anti-inflammatory cytokine, was slightly elevated 3 hours after injection of formulated miRNA; however, relative to the LPS control, this increase was mild and insufficient to reflect an actual immune response.

## Discussion

In summary, the data provide strong evidence for the safe and effective therapeutic delivery of a synthetic miRNA mimic. By reintroducing a tumor suppressor miRNA, miRNA replacement therapy seeks to restore a loss of function in cancer and to reactivate cellular pathways that drive a therapeutic response. As such, miRNA replacement therapy is distinct from other therapeutic approaches that are directed toward a gain of function, including kinase inhibitors, siRNAs, and miRNA antagonists. We hypothesize that the synthetic miR-34a mimic acts like a naturally occurring miR-34a and that it affects all mRNAs that are inherently regulated by endogenous miR-34a in normal cells for which the proper miR-34a-target interactions have evolved over a billion years. Of note, miR-34a inhibited tumor cells that are devoid of functional p53, suggesting that pathways downstream of miR-34a are sufficient to block cancer cell growth. miR-34a also inhibited tumor cells that showed normal levels of endogenous miR-34a, indicating that the therapeutic application of tumor suppressor miRNAs is not limited to replacement. This broad antioncogenic activity might be explained by the fact that miRNAs target multiple oncogenes and oncogenic pathways that cancer cells frequently become addicted to (2). Thus, the ability to affect multiple cancer pathways seems to be a key benefit of therapeutic miRNA mimics that act in accord with our current understanding of cancer as a "pathway disease" that can only be successfully treated when intervening with multiple cancer pathways (40–42). Other examples that support the concept of miRNA replacement therapy are provided by let-7, miR-16, and miR-26a, all of which can function as tumor suppressors and inhibit tumor growth in mouse models of cancer (18, 43, 44).

It is interesting to note that, although miRNAs affect a wide spectrum of genes, administration of formulated miR-34a was well tolerated. We speculate that uptake of miRNA mimics has no effect on normal cells because pathways regulated by the miRNA mimic are already activated by the endogenous miRNA in these cells. This may also suggest that targeted delivery to tumor tissues will not be necessary. The synthetic miRNA mimic is delivered systemically in a controllable formulation without the need for ectopic expression vectors and, therefore, lacks many technical challenges associated with conventional gene therapy. Although future studies are needed to address long-term efficacy and safety in higher species, our data on miR-34a highlight the utility of synthetic miRNA mimics and support the development of this new class of cancer therapeutics.

## Disclosure of Potential Conflicts of Interest

J.F. Wiggins, L. Ruffino, K. Kelnar, M. Omotola, D. Brown, and A.G. Bader are employees of Mirna Therapeutics, Inc., which develops miRNA-based therapeutics. L. Patrawala declares no competing interests.

## Acknowledgments

We thank P. Lebourgeois for pathologic analyses, S. Beaudenon and M. Winkler for critical reading of the manuscript, and J. Shelton for technical assistance.

## Grant Support

NIH grant 1R43CA134071 (A.G. Bader).

The costs of publication of this article were defrayed in part by the payment of page charges. This article must therefore be hereby marked *advertisement* in accordance with 18 U.S.C. Section 1734 solely to indicate this fact.

Received 02/23/2010; revised 04/19/2010; accepted 05/16/2010; published OnlineFirst 06/22/2010.

## References

1. Bartel DP. MicroRNAs: genomics, biogenesis, mechanism, and function. Cell 2004;116:281–97.
2. Esquela-Kerscher A, Slack FJ. Oncomirs—microRNAs with a role in cancer. Nat Rev Cancer 2006;6:259–69.
3. Calin GA, Croce CM. MicroRNA signatures in human cancers. Nat Rev Cancer 2006;6:857–66.
4. Petrocca F, Lieberman J. Micromanipulating cancer: microRNA-based therapeutics? RNA Biol 2009;6:335–40.

5. Tong AW, Nemunaitis J. Modulation of miRNA activity in human cancer: a new paradigm for cancer gene therapy? Cancer Gene Ther 2008;15:341–55.
6. Bommer GT, Gerin I, Feng Y, et al. p53-mediated activation of miRNA34 candidate tumor-suppressor genes. Curr Biol 2007;17: 1298–307.
7. Lodygin D, Tarasov V, Epanchintsev A, et al. Inactivation of miR-34a by aberrant CpG methylation in multiple types of cancer. Cell Cycle 2008;7:2591–600.
8. Tazawa H, Tsuchiya N, Izumiya M, Nakagama H. Tumor-suppressive miR-34a induces senescence-like growth arrest through modulation of the E2F pathway in human colon cancer cells. Proc Natl Acad Sci U S A 2007;104:15472–7.
9. Corney DC, Hwang CI, Matoso A, et al. Frequent downregulation of miR-34 family in human ovarian cancers. Clin Cancer Res 16:1119–28.
10. Chim C, Wong K, Qi Y, et al. Epigenetic inactivation of the miR-34a in hematological malignancies. Carcinogenesis 2010;31:745–50.
11. Gallardo E, Navarro A, Vinolas N, et al. miR-34a as a prognostic marker of relapse in surgically resected non-small-cell lung cancer. Carcinogenesis 2009;30:1903–9.
12. Calin GA, Sevignani C, Dumitru CD, et al. Human microRNA genes are frequently located at fragile sites and genomic regions involved in cancers. Proc Natl Acad Sci U S A 2004;101:2999–3004.
13. He L, He X, Lim LP, et al. A microRNA component of the p53 tumour suppressor network. Nature 2007;447:1130–4.
14. Chang TC, Wentzel EA, Kent OA, et al. Transactivation of miR-34a by p53 broadly influences gene expression and promotes apoptosis. Mol Cell 2007;26:745–52.
15. Raver-Shapira N, Marciano E, Meiri E, et al. Transcriptional activation of miR-34a contributes to p53-mediated apoptosis. Mol Cell 2007; 26:731–43.
16. Tarasov V, Jung P, Verdoodt B, et al. Differential regulation of microRNAs by p53 revealed by massively parallel sequencing: miR-34a is a p53 target that induces apoptosis and $G_1$-arrest. Cell Cycle 2007;6:1586–93.
17. Ji Q, Hao X, Zhang M, et al. MicroRNA miR-34 inhibits human pancreatic cancer tumor-initiating cells. PLoS One 2009;4:e6816.
18. Esquela-Kerscher A, Trang P, Wiggins JF, et al. The let-7 microRNA reduces tumor growth in mouse models of lung cancer. Cell Cycle 2008;7:759–64.
19. Ovcharenko D, Jarvis R, Hunicke-Smith S, Kelnar K, Brown D. High-throughput RNAi screening *in vitro*: from cell lines to primary cells. RNA 2005;11:985–93.
20. Peltier HJ, Latham GJ. Normalization of microRNA expression levels in quantitative RT-PCR assays: identification of suitable reference RNA targets in normal and cancerous human solid tissues. RNA 2008;14:844–52.
21. Mitsudomi T, Steinberg SM, Nau MM, et al. p53 gene mutations in non-small-cell lung cancer cell lines and their correlation with the presence of ras mutations and clinical features. Oncogene 1992;7:171–80.
22. Catalogue of somatic mutations in cancer. Wellcome Sanger Trust. Available from: http://www.sanger.ac.uk.
23. Barak Y, Juven T, Haffner R, Oren M. mdm2 expression is induced by wild type p53 activity. EMBO J 1993;12:461–8.
24. el-Deiry WS, Tokino T, Velculescu VE, et al. WAF1, a potential mediator of p53 tumor suppression. Cell 1993;75:817–25.
25. Nenutil R, Smardova J, Pavlova S, et al. Discriminating functional and non-functional p53 in human tumours by p53 and MDM2 immunohistochemistry. J Pathol 2005;207:251–9.
26. Soussi T, Beroud C. Assessing TP53 status in human tumours to evaluate clinical outcome. Nat Rev Cancer 2001;1:233–40.
27. Vogelstein B, Lane D, Levine AJ. Surfing the p53 network. Nature 2000;408:307–10.
28. Weil D, Garcon L, Harper M, Dumenil D, Dautry F, Kress M. Targeting the kinesin Eg5 to monitor siRNA transfection in mammalian cells. Biotechniques 2002;33:1244–8.
29. Janmaat ML, Kruyt FA, Rodriguez JA, Giaccone G. Response to epidermal growth factor receptor inhibitors in non-small cell lung cancer cells: limited antiproliferative effects and absence of apoptosis associated with persistent activity of extracellular signal-regulated kinase or Akt kinase pathways. Clin Cancer Res 2003; 9:2316–26.
30. Bartlett DW, Davis ME. Insights into the kinetics of siRNA-mediated gene silencing from live-cell and live-animal bioluminescent imaging. Nucleic Acids Res 2006;34:322–33.
31. Bartlett DW, Davis ME. Effect of siRNA nuclease stability on the *in vitro* and *in vivo* kinetics of siRNA-mediated gene silencing. Biotechnol Bioeng 2007;97:909–21.
32. Judge AD, Bola G, Lee AC, MacLachlan I. Design of noninflammatory synthetic siRNA mediating potent gene silencing *in vivo*. Mol Ther 2006;13:494–505.
33. Judge AD, Sood V, Shaw JR, Fang D, McClintock K, MacLachlan I. Sequence-dependent stimulation of the mammalian innate immune response by synthetic siRNA. Nat Biotechnol 2005;23:457–62.
34. Kleinman ME, Yamada K, Takeda A, et al. Sequence- and target-independent angiogenesis suppression by siRNA via TLR3. Nature 2008;452:591–7.
35. Ma Z, Li J, He F, Wilson A, Pitt B, Li S. Cationic lipids enhance siRNA-mediated interferon response in mice. Biochem Biophys Res Commun 2005;330:755–9.
36. Agelaki S, Tsatsanis C, Gravanis A, Margioris AN. Corticotropin-releasing hormone augments proinflammatory cytokine production from macrophages *in vitro* and in lipopolysaccharide-induced endotoxin shock in mice. Infect Immun 2002;70:6068–74.
37. Edmiston KH, Gangopadhyay A, Shoji Y, Nachman AP, Thomas P, Jessup JM. *In vivo* induction of murine cytokine production by carcinoembryonic antigen. Cancer Res 1997;57:4432–6.
38. Pickering AK, Osorio M, Lee GM, Grippe VK, Bray M, Merkel TJ. Cytokine response to infection with *Bacillus anthracis* spores. Infect Immun 2004;72:6382–9.
39. Yang B, Trump RP, Shen Y, et al. RU486 did not exacerbate cytokine release in mice challenged with LPS nor in db/db mice. BMC Pharmacol 2008;8:7.
40. Check Hayden E. Cancer complexity slows quest for cure. Nature 2008;455:148.
41. Jones S, Zhang X, Parsons DW, et al. Core signaling pathways in human pancreatic cancers revealed by global genomic analyses. Science 2008;321:1801–6.
42. Parsons DW, Jones S, Zhang X, et al. An integrated genomic analysis of human glioblastoma multiforme. Science 2008;321:1807–12.
43. Kota J, Chivukula RR, O'Donnell KA, et al. Therapeutic microRNA delivery suppresses tumorigenesis in a murine liver cancer model. Cell 2009;137:1005–17.
44. Takeshita F, Patrawala L, Osaki M, et al. Systemic delivery of synthetic microRNA-16 inhibits the growth of metastatic prostate tumors via downregulation of multiple cell-cycle genes. Mol Ther 2009;18: 181–7.